award with ICI, Welwyn Garden City, U.K.

References and Notes

(1) P.-G. de Gennes, *J. Chem. Phys.*, **55**, 572 (1971).
(2) J. D. Ferry, "Viscoelastic Properties of Polymers", 3rd ed., Wiley, New York, 1980, p 244.
(3) M. Doi, *J. Polym. Sci., Polym. Lett. Ed.*, **19**, 265 (1981).
(4) M. Doi and S. F. Edwards, *J. Chem. Soc., Faraday Trans. 2*, **74**, 1798 (1978).
(5) M. Doi and S. F. Edwards, *J. Chem. Soc., Faraday Trans. 2*, **74**, 1802 (1978).
(6) M. Doi and S. F. Edwards, *J. Chem. Soc., Faraday Trans. 2*, **74**, 1818 (1978).
(7) M. Doi and S. F. Edwards, *J. Chem. Soc., Faraday Trans. 2*, **75**, 38 (1979).
(8) W. W. Graessley, *Adv. Polym. Sci.*, **47** (1982).
(9) M. Doi and N. Y. Kuzuu, *J. Polym. Sci., Polym. Lett. Ed.*, **18**, 775 (1980).
(10) N. Metropolis, A. Rosenbluth, M. Rosenbluth, A. Teller, and E. Teller, *J. Chem. Phys.*, **21**, 6 (1953).
(11) R. B. Bird, R. C. Armstrong, O. Hassager, and C. F. Curtiss, "Dynamics of Polymeric Liquids", Wiley, New York, 1977, Vol. 1 and 2.

Effect of Cross-Bridge Motion on the Spectrum of Light Quasielastically Scattered from *Limulus* Thick Myofilament Suspensions

Satoru Fujime*† and Kenji Kubota‡

Mitsubishi-Kasei Institute of Life Sciences, Machida, Tokyo 194, Japan, and Department of Physics, Ochanomizu University, Bunkyo, Tokyo 112, Japan. *Received June 8, 1983*

ABSTRACT: A thick myofilament has many projections called cross-bridges. In order to see the effect of cross-bridge motion on the spectrum of light quasielastically scattered from suspensions of isolated thick myofilaments, a theoretical model for a semiflexible filament[2] is extended to a situation where each projection from the filament undergoes thermal fluctuations around its mean position. If activation by calcium ions would result in an increase of the flexibility of some part(s) of each projection, our simple model could account for the most part for the excess line width in the activated state over that in the relaxed/rerelaxed one observed for *Limulus* thick myofilament suspensions.[1] On the basis of the same experimental result, we estimated the flexibility parameter of the *Limulus* thick myofilament in the relaxed/rerelaxed state.

Introduction

The main aim of this paper is to discuss a possible contribution of motions of projections (cross-bridges) to the line widths of the spectra observed by Kubota et al.[1] for *Limulus* thick myofilament suspensions. Figure 1 sketches one of their results. From this figure, we know that at $K^2 = 10 \times 10^{10}$ cm^{-2}

$$\bar{\Gamma}/K^2 \simeq 6D_1 \quad \text{(in a relaxed state)}$$
$$\bar{\Gamma}/K^2 \simeq 10D_1 \quad \text{(in an activated state)}$$
$$\bar{\Gamma}/K^2 \simeq 4D_1 \quad \text{(in a rerelaxed state)} \qquad (1)$$

where $\bar{\Gamma}$ is the average line width, K is the length of the momentum transfer vector, D and D_1 are respectively the overall and the sideways translational diffusion constants of a single thick filament and $D_1 = (3/4)D$ in the long-rod limit.

In another paper,[2] we showed that the limiting form of the first cumulant, $\bar{\Gamma}$, of the correlation function $G^1(\tau)$ for a very long and semiflexible filament is given by

$$\bar{\Gamma}/K^2 \to [D - (1/3)(D_3 - D_1)] + (L^2/12)\Theta + \frac{k_BT}{\zeta L}\sum_m{}''1 \quad \text{(when } KL \gg 1) \qquad (2)$$

where $D = (2D_1 + D_3)/3$, D_3 is the lengthways translational diffusion constant of the filament, L is its length, and $\sum''1$ means the number of bending modes of motion involved in the scattering process. When we take the long-rod limit of diffusion constants, i.e., $D_3 = 2D_1$, $D - {}^1/_3(D_3 - D_1) = D_1$, $(L^2/12)\Theta = D_1$, and $k_BT/\zeta L = D_1$, eq 2 is written as

$$\bar{\Gamma}/K^2 \to D_1 + D_1 + D_1\sum_m{}''1 \quad \text{(when } KL \gg 1) \qquad (3)$$

Equation 3 tells us that each mode of motion contributes to $\bar{\Gamma}/K^2$ by D_1 in the limit of $KL \gg 1$. For a very long filament with a slight flexibility we can expect that $\sum''1 = 2$–3 at the highest accessible K value. Actually, the length of a *Limulus* thick filament is 4 μm in the relaxed state and 3 μm in the activated/rerelaxed state. Thus, we may have $\bar{\Gamma}/K^2 = (4$–$5)D_1$ at, say, $K^2 = 10 \times 10^{10}$ cm^{-2}. This estimation can explain the experimental results of thick myofilaments in the relaxed/rerelaxed state (for details, see Appendix A). On the other hand, if we try to explain $\bar{\Gamma}/K^2 = 10D_1$ on the basis of eq 3, we have to assume a nonrealistic value for the filament flexibility. Thus, we have to seek another mode of motion which gives an extra line width of about $6D_1$.

Calcium ions induce the extra line width[1]. In addition to this, the following facts have already been shown.[3,4] Congo Red, which can shorten isolated myofibrils in the relaxing solution, also increases the $\bar{\Gamma}$ value. After heat denaturation or cleavage of the S1 moiety with papain, calcium ions do not increase the $\bar{\Gamma}$ value. The dramatic increase in $\bar{\Gamma}$ is also suppressed by treating the filaments with a myosin ATPase inhibitor such as vanadate ions or by replacing ATP with Cr-ADP. These results clearly indicate that the extra line width comes mostly from an "activated" motion of cross-bridges.

In what follows, we consider a simple model where the core of the thick filament is assumed to be a rigid rod and each projection from the core fluctuates around its mean position. The former assumption does not impose any serious restriction on the present problem, because the limiting value of $\bar{\Gamma}/K^2$ is a simple sum of various contri-

† Mitsubishi-Kasei Institute of Life Sciences.
‡ Ochanomizu University.

0024-9297/84/2217-0441$01.50/0

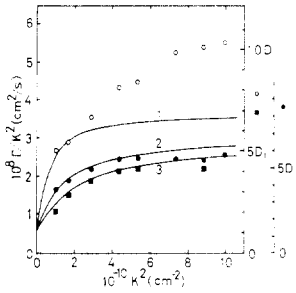

Figure 1. Typical experimental results obtained by Kubota et al.[1] The relationship of $\bar{\Gamma}/K^2$ vs. K^2 for the intensity of autocorrelation functions of scattered light from *Limulus* thick myofilament suspensions in a relaxed state (●), in an activated state (○), and in a rerelaxed state (■). $D_1 = 5.3 \times 10^{-9}$ cm^2/s for (●) and 6.4×10^{-9} cm^2/s for (○, ■), which were computed from dimensions of the filament.[1] Solid lines show simulated results (see Appendix A); curve 1 for $\gamma L = 0.2$ and $L = 3$ μm, curve 2 for $\gamma L = 0.1$ and $L = 4$ μm and curve 3 for $\gamma L = 0.05$ and $L = 4$ μm.

butions as in eq 2. The model at the present version is very crude, but it seems to be basically correct.

Model

The mass distribution along the long axis of the thick filament is assumed to be given (in terms of the molecule-fixed coordinates) by

$$m(\mathbf{r}) = m_0 S(z)\delta[x]\delta[y] + (w/N+1)\sum_j \delta[z - jb - \delta_j^z(t)]\delta[x - \delta_j^x(t)]\delta[y - \delta_j^y(t)] \quad (4)$$

where $S(z) = 1$ for $|z| \leq L/2$ and zero otherwise, $\delta[z]$ is the Dirac delta function, j runs from $-N/2$ to $N/2$, the z axis is taken to be parallel to the rod axis, and the cross-sectional area of the filament and the volume of the projection are included in m_0 and w, respectively. The integration of eq 4 over $\mathbf{r} = (x, y, z)$ gives $m_0 L + w$, which is the total mass of the rod. Thus, m_0 is the linear mass density of the core of the thick filament and w is the total mass of projections (HMM's) on a filament; $w/(N+1)$ is the mass of the single projection, $N+1$ is the total number of projections per filament, and the four projections at the same z-level were counted as one projection (Figure 2; see later). The axial repeat period of projections is denoted by b, i.e., $(N+1)b = L$, whereby the helical distribution of projections is not primarily important in the case of light scattering. The fluctuation of the jth projection around its mean position, $z = bj$, is denoted by $\delta_j(t) = [\delta_j^x(t), \delta_j^y(t), \delta_j^z(t)]$, where we assume $\langle\delta_j^x(t)\rangle = \langle\delta_j^y(t)\rangle = \langle\delta_j^z(t)\rangle = 0$ and $\langle\delta_j^x(t)^2\rangle = \langle\delta_j^y(t)^2\rangle = \langle\delta_j^z(t)^2\rangle = \langle\delta^2\rangle$ (isotropic). The scattered amplitude of light from the rod at an orientation θ, or $\xi = \cos\theta$, is given by (see Figure 2)

$$a(K,\xi,t) = (1/L)\int m(r)e^{i\mathbf{K}\cdot\mathbf{r}}\,d\mathbf{r} = m_0 j_0(k\xi) + m_1(1/N+1)\sum_j e^{i(Kb)j\xi}e^{i\mathbf{K}\cdot\delta_j(t)} \quad (5)$$

where $j_0(z)$ is the zeroth order spherical Bessel function, $m_1 = w/L$ is the averaged linear mass density of the distribution of projections on a rod, and $k \equiv KL/2$. Let us define the correlation function

$$C(K,\xi,\xi',\tau) \equiv \langle a(K,\xi,t)a^*(K,\xi',t')\rangle \quad (6)$$

where $\langle\cdots\rangle$ denotes the average over the Gaussian distribution of $\delta_j(t)$ and $\tau \equiv |t - t'|$. Now, we assume (see Appendix B)

$$\langle\delta_j(t)\cdot\delta_{j'}(t')\rangle = 3\langle\delta^2\rangle\exp(-\tau/\tau_0)f(|j-j'|) \quad (7a)$$

where τ_0 is a suitably defined correlation time and $f(|j - j'|)$ is a spatial correlation function. For simplicity of manipulation, we further assume

$$f(|j-j'|) = 1 \quad \text{for } |j-j'| \leq l$$
$$f(|j-j'|) = 0 \quad \text{for } |j-j'| > l \quad (7b)$$

where l is an integer (the correlation length). Since the average of $\exp[iz(t)]$ over the Gaussian distribution of $z(t)$ equals $\exp[-\langle z(t)^2\rangle/2]$, we have

$$\langle\exp[i\mathbf{K}\cdot\{\delta_j(t) - \delta_{j'}(t')\}]\rangle = \exp(-K^2\langle\delta^2\rangle)\exp[K^2\langle\delta^2\rangle f(|j-j'|)\exp(-\tau/\tau_0)] \quad (8)$$

From the assumption in eq 7b, it is evident that

$$\exp[K^2\langle\delta^2\rangle\exp(-\tau/\tau_0)f(|j-j'|)] - 1 = f(|j-j'|)[\exp\{K^2\langle\delta^2\rangle\exp(-\tau/\tau_0)\} - 1] \quad (9)$$

By use of the above results and eq C2 in Appendix C, eq 6 is written as

$$C(K,\xi,\xi',\tau) = (m_0 + \bar{m}_1)^2 j_0(k\xi)j_0(k\xi') + \bar{m}_1^2[\exp\{K^2\langle\delta^2\rangle\exp(-\tau/\tau_0)\} - 1]\Phi(\xi,\xi') \quad (10)$$

where

$$\bar{m}_1 = m_1\exp(-K^2\langle\delta^2\rangle/2) \quad (11)$$

$$\Phi(\xi,\xi') = (1/N+1)^2\sum_j\sum_{j'} f(|j-j'|)\exp[i(Kb)(j\xi - j'\xi')] \quad (12)$$

The field correlation function of scattered light is given by

$$G^1(\tau) = \exp[-\{D - (1/3)(D_3 - D_1)\}K^2\tau] \times (1/2)\int\int_{-1}^{1} C(K,\xi,\xi',\tau)g_K(\xi,\xi';\tau)\,d\xi\,d\xi' \quad (13)$$

where $g_K(\xi,\xi';\tau)$ is the Green function of the diffusion equation for the rotational Brownian motion of the rod, or the conditional probability that the rod will be found at an orientation ξ at time t if it is found at ξ' at time t' (ref 2).

(1) Static Intensity. Since $g_K(\xi,\xi';0) = \delta(\xi - \xi')$, we have

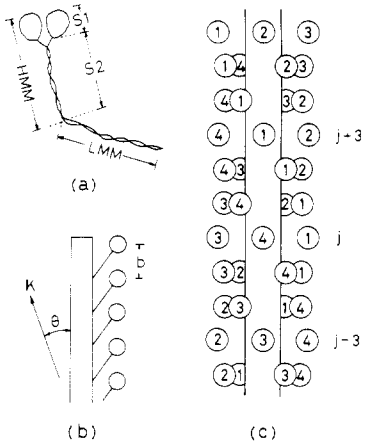

Figure 2. Schematic illustration of the structure of a thick filament. (a) A diagram of a single myosin molecule indicating the names of various regions; light meromyosin (LMM), and heavy meromyosin (HMM) which consists of subfragment 1 (S1) and subfragment 2 (S2). HMM forms a projection (or a cross-bridge) of and LMM forms a part of the core of the thick filament. (b) A model structure of a thick filament. **K** is the scattering vector, θ is the instantaneous angle between **K** and the rod axis, and b is the axial repeat period of the distribution of projections. (c) A sketch of a thick filament showing a dense distribution of projections on the surface of the core. Each circle represents two S1's of a single HMM, and S2 is not shown. The numbers attached to circles show four strands of projections. (This figure is drawn on the basis of X-ray results,[7] but the relative scale is approximate.)

$$G^1(0) = (m_0 + \bar{m}_1)^2(1/2)\int_{-1}^{1} j_0(k\xi)^2\, d\xi + m_1^2[1 - \exp(-K^2\langle\delta^2\rangle)](1/2)\int_{-1}^{1}\Phi(\xi,\xi)\, d\xi \quad (14)$$

where $(1/2)\int j_0(k\xi)^2\, d\xi = \sum_n (2n+1)b_n(k)^2$ given below and $(1/2)\int\Phi(\xi,\xi)\, d\xi = (\pi/KL)g(l)$ given in eq C5 in Appendix C. Since $j_0(k\xi) \to (\pi/k)\delta(\xi)$ as k becomes very large, we have

$$G^1(0) \to (m_0 + \bar{m}_1)^2(\pi/KL)S(0) \qquad (\text{when } KL \gg 1) \quad (15a)$$

$$S(0) = 1 + \left(\frac{m_1}{m_0 + \bar{m}_1}\right)^2 (1 - e^{-K^2\langle\delta^2\rangle})g(l) \quad (15b)$$

(2) First Cumulant $\bar{\Gamma}$ of $G^1(\tau)$. The first cumulant is given by

$$\bar{\Gamma} = -\lim \frac{\partial}{\partial\tau} \ln G^1(\tau) \quad (16)$$

where "lim" means to take the limiting value at $\tau = 0$ of its operand. When we use the short-time form of the Green function at $KL \gg 1$[2]

$$g_K(\xi,\xi';\tau) = \left[\frac{1}{4\pi\Theta\tau}\right]^{1/2} \exp\left[-\frac{(\xi - \xi')^2}{4\Theta\tau}\right] \quad (17)$$

we have (see Appendix C in ref 2 and eq C9 in Appendix C)

$$\lim \frac{\partial}{\partial\tau}\frac{1}{2}\int\int j_0(k\xi)j_0(k\xi')g_K(\xi,\xi';\tau)\, d\xi\, d\xi' \to -K^2(L^2/12)\Theta \times \pi/KL \quad (18)$$

$$\lim \frac{\partial}{\partial\tau}\frac{1}{2}\int\int \Phi(\xi,\xi')g_K(\xi,\xi';\tau)\, d\xi\, d\xi' \to -K^2(L^2/12)\Theta \times (\pi/KL)g(l) \quad (19)$$

Equation 18 comes from rotation of the core of the filament and eq 19 from rotation of the aligned projections with the core. Using eq 15, 18, and 19, we have from eq 10 and 16

$$\bar{\Gamma}/K^2 \to \left[D - \frac{1}{3}(D_3 - D_1)\right] + \frac{L^2}{12}\Theta + \left(\frac{m_1}{m_0 + \bar{m}_1}\right)^2 \frac{\langle\delta^2\rangle}{\tau_0} g(l)/S(0) \qquad (\text{when } KL \gg 1) \quad (20)$$

(3) Formal Expression of $G^1(\tau)$. For the completeness of the present model, we give the formal expression of $G^1(\tau)$. For the Green function, we use the following form[2]

$$g_K(\xi,\xi';\tau) = \sum_n \frac{(2n+1)}{2} P_n(\xi)P_n(\xi') \exp[-n(n+1)\Theta\tau] \quad (21)$$

(A more complete form of $g_K(\xi,\xi';\tau)$ is available,[2] and it is not difficult to compute $G^1(\tau)$ for that Green function.) From eq 10, 12, 13, and 21, we have

$$G^1(\tau) = e^{-DK^2\tau}\{(m_0 + \bar{m}_1)^2 \sum_{n=\text{even}} (2n+1)b_n(k)^2 e^{-n(n+1)\Theta\tau} + \bar{m}_1^2\{\exp[K^2\langle\delta^2\rangle \exp(-\tau/\tau_0)] - 1\}\sum_n a_n(k)e^{-n(n+1)\Theta\tau}\} \quad (22)$$

$$b_n(k) = (1/k)\int_0^k j_n(z)\, dz \qquad \text{for even } n \quad (23)$$

$$b_n(k) = 0 \qquad \text{for odd } n \quad (23a)$$

$$a_n(k) = (2n+1)\left(\frac{1}{N+1}\right)^2 \sum_j\sum_{j'} f(|j - j'|)j_n(Kbj)j_n(Kbj') \quad (24)$$

In eq 22, the first term in the parentheses just corresponds to the Pecora formula for rods.[5] The evaluation of $a_n(k)$ is rather tedious, but it is evident that $\sum_n a_n(k) = (\pi/KL)g(l)$ at $KL \gg 1$.

Table I
Numerical Values of $S(0) - 1$ in Eq 15b at $K^2 = 10 \times 10^{10}$ cm^{-2}

l	$\delta = 5^a$	$\delta = 15$	$\delta = 25$	$\delta = 30$
2	0.0004	0.036	0.099	0.141
3	0.0005	0.047	0.129	0.183
6	0.0007	0.062	0.171	0.243
8	0.0006	0.060	0.165	0.234

[a] δ in nm.

(4) Remarks. Throughout the present formulation, we ignored the shape factor $P(K)$ of the projection, because the size of the projection, about 10 nm in diameter of the equivalent sphere, gives $P(K)$ of about 0.98 (instead of 1.0) even at $K^2 = 10 \times 10^{10}$ cm^{-2}. This kind of neglection was made for the diameter of the core and the helical distribution of projections.

In eq 4, the four projections were implicitly assumed to move in a correlated way. However, if we take into account a dense distribution of projections on the surface of the core of the thick filament, we could accept such an assumption: The projections 1 at the jth and $(j + 3)$th z-levels (see Figure 2c) will move in a correlated way because of a strong intrastrand correlation at a large-amplitude fluctuation. The projections 1 and 4 at respectively the $(j + 3)$th and the jth z-levels will also move in a correlated way. Then, we could expect that projections 1 and 4 at the jth z-level would also move in a correlated way. From this reason, we could expect both intra- and interstrand correlation of cross-bridge motion provided that the intrastrand correlation has some correlation length $l \gtrsim 3$.

If $4(2l + 1)$ projections move in a correlated way, the friction constant in eq B1 in Appendix B should be replaced by $4(2l + 1)\zeta$ in the free-draining limit. In such a situation, we still have relationships $\tau_0 = \zeta/k = \langle\delta^2\rangle/D_{HMM}$ as they are in Appendix B, but $\langle\delta^2\rangle = k_BT/[4(2l + 1)k]$, because the elastic constant should also be replaced by $4(2l + 1)k$.

Discussion

To see the plausibility of the present model, an order of magnitude estimation is given below. We have m_0L = mass of (LMM's + paramyosin) = $13w_0 + 24w_0 = 37w_0$ and m_1L = mass of HMM's = $35w_0$ in unit of w_0 (ref 6). We also have $L = 3\ \mu$m[1] (in the activated state) and $b = 14.6$ nm.[7] The numerical values of $S(0) - 1$ are listed in Table I. From the numbers in this table, we know the contribution of cross-bridge motion to the static intensity.

In order to estimate the degree of contribution from cross-bridge motion to $\bar{\Gamma}/K^2$, we have to know the order of magnitude of the quantity $\langle\delta^2\rangle/\tau_0$. From the present model, it seems to be natural to assume a relationship $\langle\delta^2\rangle/\tau_0 = D_{HMM}$, where D_{HMM} is the diffusion constant of a single HMM in solution (see Appendix B). For the present discussion, we assume $D_{HMM} = 1.0 \times 10^{-7}$ cm^2/s at 25 °C.[8] The numerical values of the last term in eq 20 are listed in Table II in units of D_1. If we assume $l \gtrsim 2$, the estimated values for the contribution of cross-bridge motion to $\bar{\Gamma}/K^2$ are large enough to almost explain the extra line width mentioned in the Introduction.

Here, we have to consider another problem, that is, how long the correlation time τ_0 is. From the relation $\langle\delta^2\rangle = D_{HMM}\tau_0$, we know that $\tau_0 = (5\text{ nm})^2/(1.0 \times 10^{-7}\text{ cm}^2/\text{s}) = 2.5\ \mu$s and $\tau_0 = (25\text{ nm})^2/(1.0 \times 10^{-7}\text{ cm}^2/\text{s}) = 63\ \mu$s. The former time is too short compared with the channel width

Table II
Numerical Values of $[m_1/(m_0 + m_1)]^2 g(l)(D_{HMM}/D_1)/S(0)$ (the Last Term in Eq 20 in Units of D_1) at $K^2 = 10 \times 10^{10}$ cm^{-2} and τ_0 (μs)[a]

l	$\delta = 5$[b] $\tau_0 = 2.5$	$\delta = 15$ $\tau_0 = 23$	$\delta = 25$ $\tau_0 = 63$	$\delta = 30$ $\tau_0 = 90$
2	3.04	3.26	3.66	3.92
3	3.96	4.20	4.65	4.93
6	5.26	5.49	5.92	6.21
8	5.05	5.28	5.92	6.02

[a] $D_{HMM} = 1.0 \times 10^{-7}$ cm^2/s and $D_1 = 5.3 \times 10^{-9}$ cm^2/s. [b] δ in nm.

of the correlator in the experiment ($T = 5$ μs at $K^2 = 10 \times 10^{10}$ cm^{-2}); that is, the fluctuation due to motion of projections will decay within one channel width and could not be detected experimentally. On the other hand, the latter time is long enough to detect the motion of projections at $T = 5$ μs. (At $K^2 = 6 \times 10^{10}$ cm^{-2}, the observed extra line width was about $4D_1$ and the channel width at this K^2 value was $T = 10$ μs.) If we assume

$\langle\delta^2\rangle = <$ (5 nm)^2 (in the relaxed/rerelaxed state)

$\langle\delta^2\rangle =$ (15–25 nm)^2 (in the activated state)

only the "activated" motion of projections could be detected. In muscle, interfilament spacing is very narrow and each projection has very little space to move out. On the other hand, in the case of isolated filaments, each projection has a wide space to move out. In addition to this, myosin of this muscle has *calcium site(s)*, so that the situation assumed above may occur.

When one introduces an extra degree of freedom of motion, the first cumulant becomes larger by the amount contributed from that freedom. This additional contribution is weakly dependent on the flexibility parameter of that freedom, $\langle\delta^2\rangle$ in the present case. Even when $\langle\delta^2\rangle \to 0$, we have $[m_1/(m_0 + m_1)]^2 g(l) D_{HMM}$. However, the characteristic time τ_0 of the fluctuation becomes infinitely short as $\langle\delta^2\rangle \to 0$, and the extra degree of freedom contributes, by an amount far below the noise level, to the far wing of the frequency spectrum. This situation was already discussed for another model.[9] Our present model suggests that in the activated state, the flexibility of some part(s) of each projection remarkably increases, resulting in the increase of the $\langle\delta^2\rangle$ value.

The following discussion[7] may have a close connection to ours: A reversible transition between order and disorder of the bridge array (14.6-nm repeat of bridges) occurs as a function of ionic strength in the narrow range 0.12–0.17. The transition to disorder with increasing ionic strength may be associated with radial movement of bridges. If the bridge array is viewed as very labile and stabilized by electrostatic interactions, we can imagine that on activation the array could be "switched on" in a cooperative manner by changes in charge distribution on the bridges (as results of binding of calcium ions to, and hydrolysis of ATP on, each bridge in the activated state).

Concluding Remarks

In order to explain the extra line width of about $6D_1$, our model required $l \gtrsim 2$ in $g(l)$. For this "correlated" motion of cross-bridges, we have assumed a steric mechanism. But, the function $f(|j - j'|)$ will also be used to involve any kind of cooperative mechanisms between neighboring bridges. Since $g(l)$ rapidly reaches its final value of unity as l increases, we only need a relatively short range of the spatial correlation of any kind. Our estimation of the extra line width depends primarily on assumptions about the values of $\langle\delta^2\rangle$ and l. Although it was required for having a reasonable τ_0 value, the assumed value of $\langle\delta^2\rangle$ = (15–25 nm)^2 in the activated state seems to be rather large even for an isolated filament. There may be a possibility that the core of the thick filament becomes a little bit more flexible in the activated state than in the relaxed/rerelaxed one. If this increase in the filament flexibility occurs, it could contribute to the extra line width (see Figure 1). We have no firm guide for an appropriate combination of values of $\langle\delta^2\rangle$ and l. Our model seems to be promising, but at the moment, it provides only a possible explanation for the dramatic increase in the line width on activation of *Limulus* thick filaments.

According to the analysis in Appendix A, the flexibility parameter γL of the core of the thick filament is about 0.1 in the relaxed state and 0.05 in the rerelaxed one. The value of $\gamma = 0.017$–0.025 μm^{-1} is only 3–4 times smaller than that of the skeletal thin filament.[10] If we take into account the diameter of the core, $\simeq$19.5 nm,[11] we have to imagine that the *Limulus* thick filament is very flexible for a tensile force. Although speculative, a structure which gives such a filament flexibility will have some connection with shortening of the isolated filament from 4 to 3 μm on activation.

Acknowledgment. We thank Drs. B. Chu, M. M. Dewey, and S.-F. Fan of the State University of New York at Stony Brook for sending us some of their recent results prior to publication.

Appendix A. Estimation of the Flexibility of the Core

The mean square amplitude $\langle\delta_m^2\rangle$ of the lateral fluctuation of the mth mode of bending motion is given by $\langle\delta_m^2\rangle = 106 \times 10^{-10}/(2m - 1)^4$, cm^2, for $\gamma L = 0.1$ and $L = 4$ μm.[12] Thus, we have $K^2 \langle\delta_m^2\rangle \simeq 10^3/(2m - 1)^4$ at $K^2 = 10 \times 10^{10}$ cm^{-2}. It is known that if $K^2\langle\delta_m^2\rangle \gtrsim 1$, the mth mode contributes by almost D_1 to $\bar{\Gamma}/K^2$ (see Figure 5 and Table I in ref 10). From this consideration, we can expect $\sum_m{}''1 = 2$–3 or $\bar{\Gamma}/K^2 = (4$–$5)D_1$.

The field correlation function for a solution of a semiflexible filament is given by (see eq 21 in ref 10)

$$g^1(\tau) = \exp(-DK^2\tau)S(\tau)/S(0) \quad \text{(A1)}$$

$$S(\tau) = \int\int_{-L/2}^{L/2} J(s,s',\tau)\, ds\, ds' \quad \text{(A2)}$$

$$J(s,s',\tau) = \exp[-(K^2/6)\sum_m{}'\langle q_m^2\rangle \times \{Q(m,s)^2 + Q(m,s')^2 - 2Q(m,s)Q(m,s')e^{-\tau/\tau_m}\}] \quad \text{(A3)}$$

(Here we adopt our old model instead of the new one,[2] simply because the old model gives almost the same results at $KL \geq 30$ as, and is much easier in numerical computation than, the new one (see Discussion in ref 2).) The simulated correlation functions (taking m up to 8 in eq A3) were analyzed in the same way as for experimental ones.[1] Figure 1 shows some of the results, which suggests that the flexibility parameter γL of the core of the *Limulus* thick filament is about 0.1 in the relaxed state and 0.05 in the rerelaxed state. Thus, the γ value is in the range 0.025–0.017.

Appendix B. Estimation of the Relaxation Time τ_0

The random motion of a harmonically bound particle in solution is described by

$$\zeta\delta'(t) + k\delta(t) = \mathbf{F}(t) \quad \text{(B1)}$$

where ζ is the friction constant, k is the force constant and $\mathbf{F}(t)$ is the fluctuating force. From eq B1, we have

$$\langle \delta(t)\cdot\delta(t')\rangle = 3\langle\delta^2\rangle \exp(-\tau/\tau_0) \qquad \text{with } \tau_0 = \zeta/k \qquad \text{(B2)}$$

where $\langle \delta^u(t)\delta^v(t)\rangle = \langle\delta^2\rangle\delta_{uv}$ for $u, v = x, y$, and z as in the text. Equipartition of energy gives $k\langle\delta^2\rangle = k_BT$ or

$$\langle\delta^2\rangle = k_BT/k \qquad \tau_0 = \langle\delta^2\rangle/D_{HMM} \qquad \text{(B3)}$$

where $D_{HMM} = k_BT/\zeta$ is the translational diffusion constant of a single HMM in solution. *It should be noted that the elastic constant k is not that of the S2 portion of HMM but rather that coming from hinge portions between S2 and LMM and/or S2 and S1.*

Appendix C. Some Trigonometric Formulas

Using a formula

$$2\sum_{p=1}^{l}\cos(px) = \frac{\sin[(2l+1)x/2]}{\sin(x/2)} - 1 \qquad \text{(C1)}$$

we have

$$\frac{1}{N+1}\sum_{j=-N/2}^{N/2} e^{i(Kb)j\xi} = \frac{\sin[(N+1)Kb\xi/2]}{(N+1)\sin(Kb\xi/2)} \simeq j_0(k\xi) \qquad \text{(when } Kb\xi/2 \le 0.3\text{)} \qquad \text{(C2)}$$

By use of eq C1 and another formula

$$2\sum_{p=1}^{l} p\cos(px) = (l+1)\frac{\sin[(2l+1)x/2]}{\sin(x/2)} - \frac{\sin^2[(l+1)x/2]}{\sin^2(x/2)} \qquad \text{(C3)}$$

we have from eq 12

$$(N+1)^2\Phi(\xi,\xi) = (\sum_j 1)[1 + 2\sum_{p=1}^{l}\cos(Kb\xi p)] - 2\sum_{p=1}^{l} p\cos(Kb\xi p) = (N-l)\frac{\sin[(2l+1)Kb\xi/2]}{\sin(Kb\xi/2)} - \frac{\sin^2[(l+1)Kb\xi/2]}{\sin^2(Kb\xi/2)} \qquad \text{(C4)}$$

Thus, we have for $Kb\xi/2 \le 0.3$

$$(1/2)\int_{-1}^{1}\Phi(\xi,\xi)\,d\xi = (\pi/KL)g(l) \qquad \text{(C5)}$$

$$g(l) = \frac{N-l}{N+1}\frac{2}{\pi}S_1[(2l+1)Kb/2] + \frac{l+1}{N+1}\frac{2}{\pi}S_2[(l+1)Kb/2] \qquad \text{(C6)}$$

$$S_p(x) = \int_0^x\left(\frac{\sin z}{z}\right)^P dz \qquad (p = 1, 2) \qquad \text{(C7)}$$

Since $S_p(x) < 2$, the second term in eq C6 is not important for $l \ll N$. We also have for $l \ll N$ (cf. eq C4)

$$\left(\frac{1}{N+1}\right)^2\sum_j\sum_{j'} j^2 f(|j-j'|)e^{i(Kb)(j-j')\xi} = \left(\frac{1}{N+1}\right)^2 \times \{(\sum_j j^2)[1 + 2\sum_{p=1}^{l}\cos(Kb\xi p)] - 2\sum_{p=1}^{l} p\cos(Kb\xi p)\} = \frac{(N+1)^2}{12}\frac{\sin[(2l+1)Kb\xi/2]}{(N+1)\sin(Kb\xi/2)} + O(l/N^2) \qquad \text{(C8)}$$

Using this relation, we have for $Kb\xi/2 \le 0.3$

$$\frac{1}{2}\int_{-1}^{1}(\text{eq C8})\,d\xi = \frac{(N+1)^2}{12}\frac{\pi}{KL}g(l) + O(l/N^2) \qquad \text{(C9)}$$

For $b = 14.6$ nm[7] and $K^2 = 10 \times 10^{10}$ cm^{-2} ($Kb/2 = 0.230$), $g(l) = 0.146$, 0.681, 0.887, 1.176, 1.131, and 1.0 for $l = 0$, 2, 3, 6, 8, and large l ($=N$), respectively.

Registry No. Calcium, 7440-70-2.

References and Notes

(1) Kubota, K.; Chu, B.; Fan, S.-F.; Dewey, M. M.; Brink, P.; Colflesh, D. *J. Mol. Biol.* **1983**, *166*, 329.
(2) Maeda, T.; Fujime, S. *Macromolecules*, in press.
(3) Fan, S.-F.; Dewey, M. M.; Colflesh, D.; Chu, B. In "The Application of Laser Light Scattering to the Study of Biological Motion", Earnshaw, J. C., Steer, M. W., Eds.; Plenum Press: New York and London, 1983; pp 477–483.
(4) Fan, S.-F.; Dewey, M. M.; Colflesh, D.; Brink, P.; Chu, B. "Cross-Bridge Mechanism in Muscle Contraction", in press.
(5) Pecora, R. *J. Chem. Phys.* **1968**, *48*, 4162.
(6) The molecular weights of HMM and LMM of rabbit skeletal myosin are 350 000 and 130 000 daltons, respectively (Margossian, S. S.; Stafford, W. F., III; Lowey, S. *Biochemistry* **1981**, *20*, 2151). Thus, the mass ratio of HMM to LMM is $35w_0$:$13w_0$. The mass ratio of myosin to paramyosin of this muscle is about 2:1, or $48w_0$:$24w_0$ (private communication from S.-F. Fan).
(7) (a) Wray, J. S.; Vibert, P. J.; Cohen, C. *J. Mol. Biol.* **1974**, *88*, 343; (b) *Nature (London)* **1975**, *257*, 561.
(8) Fraser, A. B.; Eisenberg, E.; Kielley, W. W.; Carlson, F. D. *Biochemistry* **1975**, *14*, 2207.
(9) Stockmayer, W. H.; Burchard, W. J. *J. Chem. Phys.* **1979**, *70*, 3138.
(10) Maeda, T.; Fujime, S. *Macromolecules* **1981**, *14*, 809.
(11) Levine, R. J. C.; Dewey, M. M.; Devillafranca, G. W. *J. Cell. Biol.* **1972**, *55*, 221.
(12) Fujime, S. *J. Phys. Soc. Jpn.* **1971**, *31*, 1805.